Dielectric back scattering patterns for light trapping in thin-film Si solar cells

M. van Lare,[1,*] F. Lenzmann,[2] and A. Polman[1]

[1]*Center for Nanophotonics, FOM Institute AMOLF Science Park 104, 1098 XG, Amsterdam, The Netherlands*
[2]*Energy Research Center of The Netherlands ECN, P. O. Box 1, 1755 ZG Petten, The Netherlands*
[*]*lare@amolf.nl*

Abstract: We experimentally compare the light trapping efficiency of dielectric and metallic backscattering patterns in thin-film a-Si:H solar cells. We compare devices with randomly patterned Ag back contacts that are covered with either flat or patterned aluminum-doped ZnO (AZO) buffer layers and find the nanostructure at the AZO/a-Si:H interface is key to achieve efficient light trapping. Simulations show that purely dielectric scattering patterns with flat Ag and a patterned AZO/a-Si:H interface can outperform geometries in which the Ag is also patterned. The scattering from the dielectric patterns is due to geometrical Mie resonances in the AZO nanostructures. The optimized dielectric geometries avoid parasitic Ohmic losses due to plasmon resonances in the Ag, and open the way to a large number of new light trapping designs based on purely dielectric resonant light scattering.

OCIS codes: (040.5350) Photovoltaic; (290.4020) Mie theory.

References and links

1. J. Zhu, C.-M. Hsu, Z. Yu, S. Fan, and Y. Cui, "Nanodome solar cells with efficient light management and self-cleaning," Nano Lett. **10**(6), 1979–1984 (2010).
2. R. Biswas, J. Bhattacharya, B. Lewis, N. Chakravarty, and V. Dalal, "Enhanced nanocrystalline silicon solar cell with a photonic crystal backreflector," Sol. Energy Mater. Sol. Cells **94**(12), 2337–2342 (2010).
3. O. Isabella, A. Campa, M. C. R. Heijna, W. Soppe, R. Van Erven, R. H. Franken, H. Borg, and M. Zeman,S. Valencia, ed., "Diffraction Grating for Light Trapping in Thin-Film Silicon Solar Cells", in *Proceedings of the 23rd European Photovoltaic Solar EnergyConference*, ed. (Valencia, Spain, 2008), p 2320–2324.
4. S. B. Mallick, M. Agrawal, and P. Peumans, "Optimal light trapping in ultra-thin photonic crystal crystalline silicon solar cells," Opt. Express **18**(6), 5691–5706 (2010).
5. H. A. Atwater and A. Polman, "Plasmonics for improved photovoltaic Devices," Nat. Mater. **9**(3), 205–213 (2010).
6. V. E. Ferry, M. A. Verschuuren, M. C. Lare, R. E. I. Schropp, H. A. Atwater, and A. Polman, "Optimized Spatial Correlations for Broadband Light Trapping Nanopatterns in High Efficiency Ultrathin Film a-Si:H Solar Cells," Nano Lett. **11**(10), 4239–4245 (2011).
7. C. Eisele, C. E. Nebel, and M. Stutzmann, "Periodic light coupler gratings in amorphous thin film solar cells," J. Appl. Phys. **89**(12), 7722 (2001).
8. R. H. Franken, R. L. Stolk, H. Li, C. H. M. van der Werf, J. K. Rath, and R. E. I. Schropp, "Understanding light trapping by light scattering textured back electrodes in thin film n-i-p-type silicon solar cells," J. Appl. Phys. **102**(1), 014503 (2007).
9. C. Rockstuhl, S. Fahr, K. Bittkau, T. Beckers, R. Carius, F.-J. Haug, T. Söderström, C. Ballif, and F. Lederer, "Comparison and optimization of randomly textured surfaces in thin-film solar cells," Opt. Express **18**(S3 Suppl 3), A335–A341 (2010).
10. D. Shir, J. Yoon, D. Chanda, J. H. Ryu, and J. A. Rogers, "Performance of ultrathin silicon solar microcells with nanostructures of relief formed by soft imprint lithography for broad band absorption enhancement," Nano Lett. **10**(8), 3041–3046 (2010).
11. C. Battaglia, J. Escarré, K. Söderström, M. Charrière, M. Despeisse, F.-J. Haug, and C. Ballif, "Nanomoulding of transparent zinc oxide electrodes for efficient light trapping in solar cells," Nat. Photonics **5**(9), 535–538 (2011).
12. V. E. Ferry, M. A. Verschuuren, H. B. T. Li, E. Verhagen, R. J. Walters, R. E. I. Schropp, H. A. Atwater, and A. Polman, "Light trapping in ultrathin plasmonic solar cells," Opt. Express **18**(S2 Suppl 2), A237–A245 (2010).

#191050 - $15.00 USD Received 23 May 2013; revised 2 Aug 2013; accepted 12 Aug 2013; published 28 Aug 2013

13. C. Rockstuhl, S. Fahr, and F. Lederer, "Absorption enhancement in solar cells by localized plasmon polaritons," J. Appl. Phys. **104**(12), 123102 (2008).
14. P. Spinelli, V. E. Ferry, J. van de Groep, M. van Lare, M. A. Verschuuren, R. E. I. Schropp, H. A. Atwater, and A. Polman, "Plasmonic light trapping in thin-film solar cells," J. Opt. **14**(2), 024002 (2012).
15. A. Williamson, É. McClean, D. Leipold, D. Zerulla, and E. Runge, "The design of efficient surface-plasmon-enhanced ultra-thin polymer-based solar cells," Appl. Phys. Lett. **99**(9), 093307 (2011).
16. F. J. Beck, E. Verhagen, S. Mokkapati, A. Polman, and K. R. Catchpole, "Resonant SPP modes supported by discrete metal nanoparticles on high-index substrates," Opt. Express **19**(Suppl 2), A146–A156 (2011).
17. M. van Lare, F. Lenzmann, M. A. Verschuuren, and A. Polman, "Mode coupling by plasmonic surface scatterers in thin-film silicon solar cells," Appl. Phys. Lett. **101**(22), 221110 (2012).
18. Y. A. Akimov and W. S. Koh, "Design of Plasmonic Nanoparticles for Efficient Subwavelength Light Trapping in Thin-Film Solar Cells," Plasmonics **6**(1), 155–161 (2011).
19. K. R. Catchpole and A. Polman, "Plasmonic solar cells," Opt. Express **16**, 21793 (2008).
20. V. Jovanov, U. Planchoke, P. Magnus, H. Stiebig, and D. Knipp, "Influence of back contact morphology on light trapping and plasmonic effects in microcrystalline silicon single junction and micromorph tandem solar cells," Sol. Energy Mater. Sol. Cells **110**, 49–57 (2013).
21. U. W. Paetzold, E. Moulin, D. Michaelis, W. Böttler, C. Wächter, V. Hagemann, M. Meier, R. Carius, and U. Rau, "Plasmonic reflection grating back contacts for microcrystalline silicon solar cells," Appl. Phys. Lett. **99**(18), 181105 (2011).
22. P. Spinelli, M. A. Verschuuren, and A. Polman, "Broadband omnidirectional antireflection coating based on subwavelength surface Mie resonators," Nat. Commun. **3**, 692 (2012).
23. C. f. Bohren and D. R. Huffman, *Absorption and Scattering of Light by Small Particles* (Wiley, New York, 2008).
24. W. J. Soppe, H. Borg, B. B. Van Aken, C. Devilee, M. Dörenkämper, M. Goris, M. C. R. Heijna, J. Löffler, and P. Peeters, "Roll to roll fabrication of thin film silicon solar cells on nano-textured substrates," J. Nanosci. Nanotechnol. **11**(12), 10604–10609 (2011).

1. Introduction

Thin film solar cells, with absorber layer thicknesses ranging from a few hundred nanometers to a few microns, combine the advantages of relatively low fabrication cost with the possibility to realize mechanically flexible devices. However, the small absorber layer thickness leads to poor absorption of the infra-red part of the solar spectrum, in particular in solar cells based on amorphous and microcrystalline silicon thin films due to the unfavourable charge carrier mobilities and lifetimes in these materials. To solve this problem, light trapping is required, in which nanostructures incorporated in the solar cell are designed to scatter the light and thereby enhance the optical path length. Many different periodic and random scattering geometries have been proposed in order to achieve efficient light trapping over a broad spectral range [1–21]. Several device designs make use of the efficient scattering properties of metallic nanoparticles, which have large scattering cross sections at their plasmon resonance [6, 12–21].

Recently, it was shown that dielectric nanostructures on top of a solar cell can lead to strongly enhanced light incoupling due to forward scattering through resonantly excited Mie modes in the nanoparticles [6,22]. Similar to plasmonic nanostructures, these dielectric surface nanostructures are very efficient resonant scatterers with scattering cross sections exceeding their geometrical cross sections [22,23]. Moreover, dielectric scattering structures show much lower parasitic absorption than metallic nanostructures [20].

Many research groups have now demonstrated efficient broadband light trapping in thin-film devices grown on top of structured metal back contacts [6,12,20,21]. In the case of thin-film Si solar cells, the metallic back contact is always separated from the absorber layer by an aluminium doped ZnO (AZO) layer, to avoid metal diffusion into the Si. Such a geometry is shown in Fig. 1(a), which shows a cross-section made using focused ion beam (FIB) milling. Here, a randomly patterned glass substrate is covered with a thin Ag layer, on top of which subsequent layers of AZO, a-Si:H and indium-tin-oxide (ITO) are deposited. Due to conformal growth of the AZO layer on top the structured back contact, the AZO layer also contains the nanostructures. The solar cell is thus composed of random scattering patterns at both the Ag/AZO and the AZO/a-Si:H interface.

#191050 - $15.00 USD Received 23 May 2013; revised 2 Aug 2013; accepted 12 Aug 2013; published 28 Aug 2013

A natural question now arises if the light trapping in these solar cells is due to scattering from plasmon resonances in the Ag or from Mie resonances in the AZO nanostructures. Deciphering the effect of both scattering structures is important for a large number of thin-film solar cell designs. In this paper we systematically study the influence of the structured AZO layer on light trapping in thin-film Si solar cells grown on top of a structured metal back contact.

We experimentally compare thin-film a-Si:H devices with structured Ag and either structured or flat AZO layers. We show that flattening the AZO buffer layer is detrimental for light trapping, demonstrating the key importance of dielectric scattering for light trapping even in plasmonic geometries. We study both random and periodic structures and demonstrate examples of purely dielectric scattering patterns.

2. Sample fabrication

The solar cell fabrication was performed as described by Soppe *et al.* [24]. Flat glass substrates and Asahi U-type substrates were sputter-coated with a 200 nm Ag layer and an AZO buffer layer. An a-Si:H layer (350 nm i-layer) was then grown using plasma-enhanced chemical vapour deposition (PECVD) in *n-i-p* configuration. To define the different cell areas 4 × 4 mm pads of ITO were sputtered on top of the a-Si:H layer using a contact mask. Finally U-shaped Ag contacts were sputtered on top through a contact mask.

Figure 1 shows cross sections, made using focused ion beam (FIB) milling, of the different types of cell geometries that were compared. Figure 1(a) shows the "standard" geometry in which the cell is grown on top of an Asahi *-type substrate and has an 80 nm AZO layer. Next to the "standard" geometry, three complementary geometries were made. One cell type was grown on top of a flat glass substrate and has an AZO thickness of approximately 500 nm (Fig. 1(b)). One cell type was grown on top of an Asahi U-type substrate and also has a 500 nm AZO layer (Fig. 1(c)). This results in roughness in both the Ag/AZO layer and the AZO/a-Si:H interface. And one cell type was made by depositing AZO onto Asahi U-type substrate and then polishing the AZO surface using chemical mechanical polishing with colloidal SiO_2 slurry. This resulted in a sample with structured Ag/AZO interface and a flat AZO/a-Si:H interface (Fig. 1(d)). The use of a rather thick (500 nm) AZO layer enabled polishing without exposing the Ag. A total of 24 cells were made of each type, so that electrical cell parameters could be averaged in the analysis. AFM data of Ag coated Asahi U-type substrates are shown in ref [6].

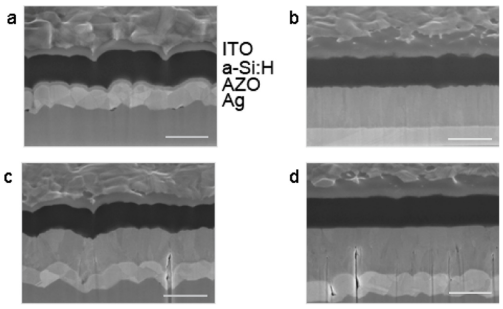

Fig. 1. FIB cross sections of the different cell types: (a) Reference a-Si:H solar cell, composed of an Asahi U-type substrate covered with 200 nm Ag, 80 nm AZO, 350 nm a-Si:H and ITO. (b-d) Solar cells grown on top of: (b) a flat substrate, (c) Asahi substrate with 500 nm AZO, and (d) Asahi substrate with polished AZO. Scale bars: 500 nm.

3. Experimental results

Figure 2 shows current-voltage (I-V) measurements for the four different types of cells; curves are shown for single cells. I-V curves were measured under one-sun illumination using a WACOM solar simulator. Table 1 summarizes the average open circuit voltage (V_{oc}) and

#191050 - $15.00 USD Received 23 May 2013; revised 2 Aug 2013; accepted 12 Aug 2013; published 28 Aug 2013

fill factor (FF) of the different cell types. From these measurements, no significant difference in V_{oc} and FF can be observed between the different types of cells, indicating similar electrical quality of the different device types. The curves were normalized to the current obtained from external quantum efficiency measurements at short circuit to exclude inaccuracies in the determination of the surface area of the cells. The flat cell (black) shows a photocurrent of J_{sc} = 10.7 mA/cm^2. The Asahi cells show significantly higher photocurrent. We find J_{sc} = 12.5 and 12.4 mA/cm^2 for the cells with 80 and 500 nm AZO, respectively (green, blue). The Asahi cell with polished AZO however (red), has a substantially lower photocurrent, than the normal Asahi cells: J_{sc} = 10.9 mA/cm^2. This indicates that the dielectric nanostructure at the AZO/a-Si:H interface is crucial for efficient light trapping.

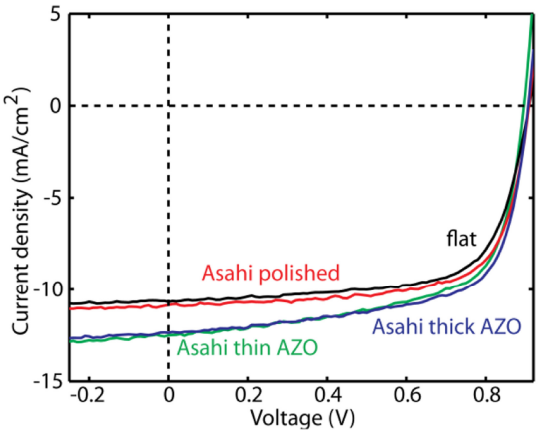

Fig. 2. I-V curves for a-Si:H cells made on flat substrate (black), Asahi substrate with 500 nm AZO (blue), Asahi substrate with 80 nm AZO (green), and Asahi substrate with polished AZO (red).

Figure 3(a) shows external quantum efficiency (EQE) measurements on the four different types of cells; measurements are shown for single cells. The EQE measurements were performed on a commercial spectral response set-up by Optosolar (SR300) using a 250 W xenon lamp equipped with a Jobin Yvon iHR320 monochromator. The diameter of the beam on the sample surface was 1 mm. The setup was calibrated with a crystalline silicon reference solar cell and the measurements were carried out with a spectral resolution of 10 nm.

The EQE for the flat solar cell (black) decreases rapidly above 550 nm, because of poor light absorption in this spectral range. The Asahi cells with structured AZO/a-Si:H interface (blue and green) show a significantly enhanced red-response with respect to the flat cell. This indicates that light trapping occurs due to the scattering nanostructures. In contrast, the Asahi cell with polished AZO shows barely any enhancement with respect to the flat cell. This shows that only structuring the Ag layer does not lead to any significant light trapping in this device geometry; i.e. the AZO/a-Si:H interface needs to be structured as well. All different types of cells show a similar highly reproducible blue response, indicating that roughness on the top, present because of conformal growth, does not play a role in the light management in these cells.

Table 1. Electrical properties of the four types of solar cells

Sample	V_{oc} (mV)	FF
Flat substrate	905 ± 7	0.68 ± 0.04
Asahi thin AZO	898 ± 15	0.66 ± 0.04
Asahi thick AZO	895 ± 16	0.64 ± 0.04
Asahi polished AZO	907 ± 12	0.69 ± 0.07

#191050 - $15.00 USD Received 23 May 2013; revised 2 Aug 2013; accepted 12 Aug 2013; published 28 Aug 2013

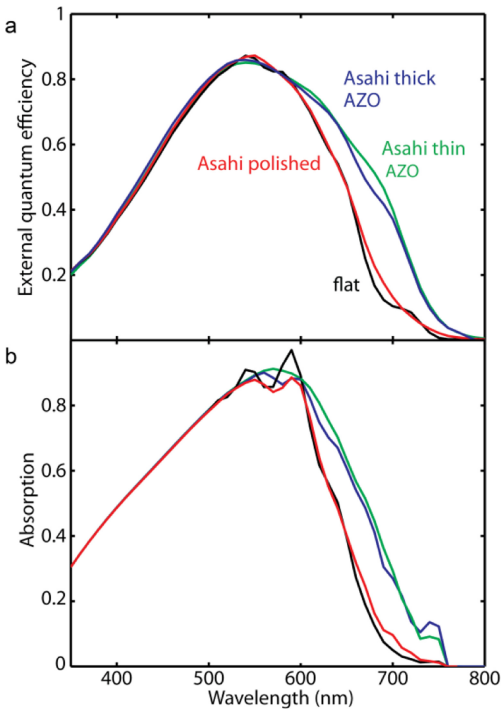

Fig. 3. (a) External quantum efficiency measurements on solar cells on a flat substrate (black), Asahi substrates with 80 nm rough AZO (green), 500 nm rough AZO (blue), and 500 nm polished AZO (red). (b) Simulated absorption in the a-Si:H layer of the same cell types (line colours correspond to those in (a)).

4. Simulations

Three-dimensional finite-difference time-domain (FDTD) simulations, performed using Lumerical software, were used to model the absorption in the a-Si:H layer. The simulations took into account the full layer structure: 200 nm Ag, 80/500 nm AZO, 350 nm a-Si:H, and 80 nm ITO. The Asahi roughness was incorporated by measuring the surface topography using atomic force microscopy (AFM) on an Asahi substrate that was sputter-coated with 200 nm Ag. The AFM data were then imported in the simulation to represent to topography of the Ag surface. In the case of the non-polished Asahi cells, the roughness of the AZO layer was assumed to be the same as the measured roughness of the Ag layer. Considering the similarity in the measured blue-response for the different types of cells with the flat and patterned AZO layers, the top of the a-Si:H layer and the ITO layer were assumed to be flat in the simulations. Periodic boundaries were used in x and y direction and a unit cell size of 2 × 2 μm was used. No effects of periodicity were observed for this size. A uniform mesh of 5 nm was used over the whole simulation volume. Perfectly matched layers were used at the top and bottom of the simulation volume.

Figure 3(b) shows the simulated fraction of incident light that is absorbed in the a-Si:H layer as a function of wavelength for the different types of cells. The simulations show very similar trends as the measured EQE data. The Asahi cells with patterned AZO (green and blue) show a significant absorption enhancement with respect to the flat cell (black) in the wavelength range above 600 nm, whereas the sample with polished AZO (red) does not. We found that making the Ag rough results in significantly higher parasitic absorption. Whereas with flat Ag, the absorption in the Ag stays below 5% over the 350-800 nm wavelength range, the absorption in the rough Ag layer is up to 50% at wavelengths above 700 nm. Considering the good agreement between our FDTD simulations and EQE measurements, next we used

#191050 - $15.00 USD Received 23 May 2013; revised 2 Aug 2013; accepted 12 Aug 2013; published 28 Aug 2013

the FDTD simulations to study the influence of the AZO layer thickness on the absorption for devices with rough Ag and polished AZO.

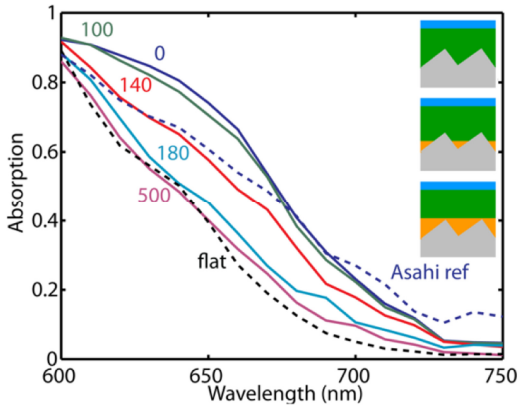

Fig. 4. Simulated absorption in the a-Si:H layer of a solar cell without roughness (black dashed, "flat"), with Asahi roughness in the Ag and AZO layer (blue, dashed, "Asahi ref."), and with Asahi roughness in the Ag and flat AZO (continuous) with a thickness of 0 nm (blue), 100 nm (green), 140 nm (red), 180 nm (light blue), and 500 nm (purple). The insets show cartoons of the different geometries with flat AZO (grey: Ag; orange: AZO; green: a-Si:H); no AZO (top), AZO thinner than Ag roughness (center), AZO thicker than Ag roughness (bottom).

Figure 4 shows the simulated absorption in the a-Si:H layer for different thicknesses of a flat AZO layer that is on top of the rough Ag. Data for a flat cell (black, dashed) and an Asahi cell with rough AZO (blue, dashed) are also shown as reference. When there is no AZO present (blue continuous, 0 nm), the rough Ag is directly in contact with the a-Si:H layer (first inset). As can be seen in the figure, this leads to efficient light trapping. At wavelengths between 600 and 680 nm, the absorption in the a-Si:H layer is even higher than for the Asahi reference (blue dashed), in which both the Ag and the AZO are rough. For the cell with flat AZO/a-Si:H interface the following trend is observed. When the AZO thickness increases to 100 nm (green), the AZO starts to fill up the valleys in the rough Ag (second inset); the areal fraction of Ag that is in direct contact with the a-Si:H rear interface is still high (72%). In this case, absorption in the a-Si:H slightly decreases with respect to the case where there is no AZO present. With 140 nm AZO (red), the fraction of Ag at the a-Si:H rear interface is only 27%, and absorption has decreased significantly. Further increasing the AZO thickness to 180 nm (light blue), leads to reduced light trapping. At an AZO layer thickness of 500 nm (purple), only very slight light trapping is observed. The data in Fig. 4 show that roughness at the a-Si:H rear interface is required for efficient light trapping in this solar cell geometry.

#191050 - $15.00 USD Received 23 May 2013; revised 2 Aug 2013; accepted 12 Aug 2013; published 28 Aug 2013

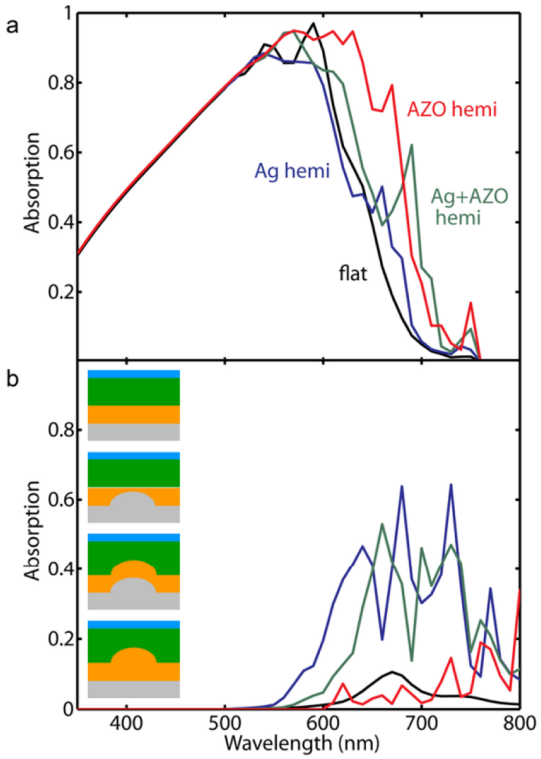

Fig. 5. (a) Simulated absorption in the a-Si:H layer of solar cells with only flat layers (black), periodically structured Ag and flat AZO (blue, "flat hemi"), periodically structured Ag and AZO (green, "Ag+AZO hemi"), flat Ag and periodically structured AZO (red, "AZO hemi"). The insets show (from top to bottom): flat cell, cell with Ag hemispheres, cell with Ag and AZO hemispheres, cell with AZO hemispheres and flat Ag.

To further investigate the loss and light trapping processes in the various geometries we have performed FDTD simulations on periodically patterned nanostructures. Such geometries are readily made using large-area inexpensive soft imprint techniques as we have demonstrated earlier [6]. Square arrays of hemispheres with a radius of 150 nm were used, using a 400 nm × 400 nm unit cell. Figure 5(a) shows the simulated absorption in the active layer of a-Si:H cells on top of periodic arrays of hemispheres in only the Ag (blue), both Ag and AZO (green) and only in the AZO (red), compared to a flat cell (black). These geometries are schematically depicted in Fig. 5(b).

Figure 5(a) shows the simulated fraction of light absorbed in the a-Si:H layer for the four geometries. The device with structured Ag and flat AZO shows poor light trapping. At wavelengths above 650 nm there is a only small enhancement in absorption with respect to the flat cell, while at wavelengths below 650 nm the Ag pattern results in a reduced absorption. When both the Ag and the AZO layer are periodically structured, a substantial amount of light trapping is observed. The device with flat Ag and patterned AZO shows even higher absorption than the cell with structured Ag and structured AZO. To study this further, we have simulated the fraction of light that is absorbed in the Ag for the different device structures (Fig. 5(b)). For structured Ag (blue and green) absorption in the Ag is significantly higher than for geometries with flat Ag (black and red), due to resonant scattering by the plasmonic nanostructures. The data in Fig. 5 show that light trapping using purely dielectric scattering patterns can be better than with combined dielectric-metallic scattering patterns, since it leads to lower parasitic absorption in the metal.

#191050 - $15.00 USD Received 23 May 2013; revised 2 Aug 2013; accepted 12 Aug 2013; published 28 Aug 2013

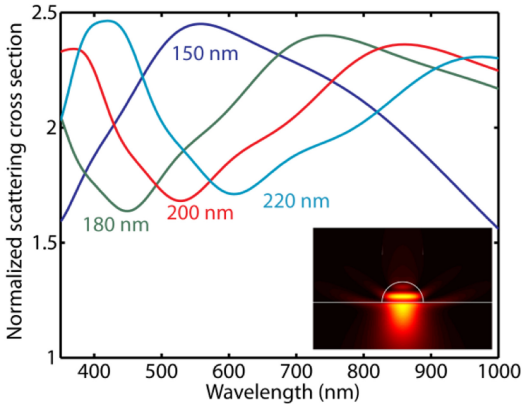

Fig. 6. Simulated normalized scattering cross sections for AZO hemispheres on a non-absorbing AZO, inside non-absorbing a-Si:H, for radii of 150 nm (blue), 180 nm (green), 200 nm (red), 220 nm (light blue). The inside shows a cross section of the field intensity.

To study the scattering mechanism from the patterned AZO/a-Si:H interface, we consider the geometrical Mie resonances in the resonant cavities at the interface. Figure 6 shows the simulated normalized scattering cross sections, defined as the ratio between the scattering cross section and the geometrical cross section, for a geometry composed of an AZO substrate with a single AZO hemisphere embedded in a-Si:H layer (see inset in Fig. 6). Data are shown for hemisphere radii in the range 150-220 nm. Optical constants for AZO and a-Si:H were used as before, but neglecting absorption (*i.e.* setting the imaginary parts of the refractive index to zero). A 2 μm × 2 μm simulation box was used with perfectly matched layers on all boundaries. A total-field-scattered-field source was used to directly calculate the scattered power by means of frequency-domain transmission monitors positioned in the scattered field region. The normalized scattering cross section for the hemisphere with 150 nm radius (blue, same size as in Fig. 5), shows a broad peak centred around 560 nm. The normalized scattering cross section exceeds unity over the entire 350-1000 nm spectral band, indicating strong interaction with the incident light. The inset shows the electric field intensity in the geometry with a 150 nm hemisphere, demonstrating the light is resonantly confined in the particle, with clear extension of the trapped resonant mode into the AZO and a-Si:H layers. We ascribe the large bandwidth of the resonance to the high loss rate associated with the enhanced leakage radiation to the AZO and a-Si:H layers. Figure 6 shows that when the particle radius is increased, the resonance shifts to higher wavelengths; further confirming the resonant Mie nature of the scattering mechanism. For the larger particles a second (higher-order) Mie resonance appears, in correspondence with the analytical Mie formulas for spherical particles. Simulated absorption for the full device geometry shows a strong size dependence; particles with a radius below 100 nm resulted in poor absorption enhancement. This indicates that geometrical resonances play an important role in the scattering process.

5. Conclusion

We have systematically compared dielectric and metallic scattering patterns for light trapping in thin Ag/AZO/a-Si:H solar cells. We experimentally demonstrate that geometries with patterned AZO buffer layers lead to substantially better light trapping than geometries with only patterned Ag. Simulations show that, if the AZO layer fills up the valleys of the rough Ag, this result is mostly independent of the AZO thickness and that structuring the AZO/a-Si:H interface is crucial for light trapping. We show that purely dielectric scattering patterns can outperform geometries in which the Ag is also structured by reducing the parasitic absorption that arises from plasmon resonances in nanostructured Ag. The light trapping with dielectric scattering patterns relies on geometrical resonances in the AZO nanostructures. Our

#191050 - $15.00 USD Received 23 May 2013; revised 2 Aug 2013; accepted 12 Aug 2013; published 28 Aug 2013

work opens the way to a large number of new light trapping designs based on dielectric resonant light scattering.

Acknowledgments

We are grateful to Maarten Dorenkamper and Klaas Bakker (ECN) for the solar cell fabrication and support with the EQE measurements. SARA Computing and Networking Services is acknowledged for support in using the Lisa Compute Cluster. This work is part of the research program of FOM, which is financially supported by NWO. It is also funded by the European Research Council, the Global Climate and Energy Project (GCEP) and NanoNextNL, a technology program of the Dutch Ministry of Economy Affairs.

#191050 - $15.00 USD Received 23 May 2013; revised 2 Aug 2013; accepted 12 Aug 2013; published 28 Aug 2013